STEM CELLS AND DEVELOPMENT
Volume 21, Number 13, 2012

DOI: 10.1089/scd.2011.0615

Tailored Integrin–Extracellular Matrix Interactions to Direct Human Mesenchymal Stem Cell Differentiation

Jessica Ellen Frith,[1,*] Richard James Mills,[1,*] James Edward Hudson,[1] and Justin John Cooper-White[1,2]

Integrins provide the primary link between mesenchymal stem cells (MSCs) and their surrounding extracellular matrix (ECM), with different integrin pairs having specificity for different ECM molecules or peptide sequences contained within them. It is widely acknowledged that the type of ECM present can influence MSC differentiation; however, it is yet to be determined how specific integrin–ECM interactions may alter this or how they change during differentiation. We determined that human bone marrow–derived mesenchymal stem cells (hMSCs) express a broad range of integrins in their undifferentiated state and show a dramatic, but transient, increase in the level of α5 integrin on day 7 of osteogenesis and an increase in α6 integrin expression throughout adipogenesis. We used a nonfouling polystyrene-block-poly(ethylene oxide)-copolymer (PS-PEO) surface to present short peptides with defined integrin-binding capabilities (RGD, IKVAV, YIGSR, and RETTAWA) to hMSCs and investigate the effects of such specific integrin–ECM contacts on differentiation. hMSCs cultured on these peptides displayed different morphologies and had varying abilities to differentiate along the osteogenic and adipogenic lineages. The peptide sequences most conducive to differentiation (IKVAV for osteogenesis and RETTAWA and IKVAV for adipogenesis) were not necessarily those that were bound by those integrin subunits seen to increase during differentiation. Additionally, we also determined that presentation of RGD, which is bound by multiple integrins, was required to support long-term viability of hMSCs. Overall we confirm that integrin–ECM contacts change throughout hMSC differentiation and show that surfaces presenting defined peptide sequences can be used to target specific integrins and ultimately influence hMSC differentiation. This platform also provides information for the development of biomaterials capable of directing hMSC differentiation for use in tissue engineering therapies.

Introduction

Tissue engineering involves the integration of functional biomaterial scaffolds and cells for the restoration of damaged or diseased tissue. Human bone marrow–derived mesenchymal stem cells (hMSCs) have attracted much attention as an ideal cell source for a multitude of tissue engineering applications, due to their relative ease of expansion, broad differentiation potential, and immuno-privileged status [1–3]. Understanding how hMSCs interpret the surfaces presented throughout a biomaterial scaffold is thus primary to the successful development of viable tissue engineering therapies.

hMSCs interact with such surfaces predominantly through integrins, cell surface receptors that bind to specific extracellular matrix (ECM) motifs, that link the cell to it's surrounding physical environment. Integrins bind to their ligand as a heterodimer comprised of both alpha and beta subunits and it is through the varying combinations of these 18 alpha and 8 beta subunits that specificity for different ECM motifs is achieved [4]. Binding of these integrins to the ECM induces a conformational change in the cytoplasmic region of beta-integrin subunits and initiates integrin clustering [5,6]. This acts as a core to which additional proteins (including talin, vinculin, and α-actinin) are recruited, all of which contain binding sites for actin, thus forming a focal adhesion [7,8]. In this way integrins, through the assembly of focal adhesions, connect the ECM to the intracellular actin cytoskeleton. In addition to these proteins, a large array of signaling proteins, such as focal adhesion kinase (FAK), Rho, Rac, and integrin-linked kinase (ILK), are also recruited [9–11]. Their functions include both regulation of cytoskeletal remodeling and the assembly or disassembly of the focal adhesion complex [9,10,11], but they also tie into intracellular signaling cascades, such as mitogen-activated protein kinase and C-Jun N-terminal kinase (JNK) [14–16], thereby

[1]Tissue Engineering and Microfluidics Laboratory, Australian Institute for Bioengineering and Nanotechnology, University of Queensland, St. Lucia, Queensland, Australia.
[2]Faculty of Engineering, Architecture and IT, School of Chemical Engineering, University of Queensland, St. Lucia, Queensland, Australia.
*These authors contributed equally to this work.

providing a point of convergence for signals generated via adhesion, to pathways activated in response to growth factor signaling. This facilitates integration of a signal, initially generated from integrin–ECM binding, to intracellular cascades and can ultimately lead to changes in gene expression, and consequently, cell behavior.

Although a number of studies have analyzed naive hMSC integrin expression, many concentrate on specific subunits. Studies that survey a more comprehensive panel have resulted in several (often contradictory) expression profiles. Gronthos et al. [17] showed that hMSCs express integrins α1β1, α2β1, α5β1, α6β1, αVβ3, and αVβ5. However, other studies have also shown that α3β1 [18,19] as well as β2 and β4 subunits may also be expressed [18,20]. Further, a recent microarray analysis demonstrated additional transcription of integrins α11, α*X*, β7, and β8 [21]. In terms of hMSC differentiation, the majority of interest has focused on determining the expression pattern throughout chondrogenesis and resolving the changes that occur during chondrocyte dedifferentiation [22–24]. Less attention has focused on osteogenic differentiation and most information has been gathered using cell lines or committed osteoblasts rather than primary hMSCs. The available evidence suggests that osteogenesis may be dependent upon the activity of β1 integrin [17] that can partner with multiple α subunits, although there are suggestions that α5 integrin, which is induced by the osteogenic factor dexamethasone, may also be important [25,26]. Similarly, adipogenic differentiation of hMSCs has not been characterized and data are only available from preadipocyte cell lines [27].

As integrins provide the primary link between cells and their matrix, the composition of the ECM (which facilitates binding of specific integrin pairs) is also a key aspect when determining the optimal conditions for hMSC differentiation. To date, ECM proteins have been shown to have varying abilities to support osteogenic [18,28–32] or adipogenic [33] differentiation of hMSCs and attempts have been made to determine the specific ECM motifs involved. However, the ECM is structurally complex with components that contain repeating units, as well as multiple adhesion motifs, whose presentation can greatly affect cell outcomes. Martino et al. [34] showed that different domains of fibronectin had varying abilities to promote osteogenesis through differing affinity for integrins α5β1 and αVβ3, and the switch between native and denatured conformations of collagen-I and collagen-IV has been shown to influence osteogenesis [35] and adipogenesis [33], respectively. Together with the limited understanding of integrin expression changes during hMSC differentiation, this makes it very difficult to determine (and therefore optimize for tissue engineering strategies) the specific integrin–ligand interactions responsible.

We hypothesized that by gaining a clear understanding of the changes to both hMSC integrin expression and ECM composition during differentiation, biomaterials could be tailored to match such changes and thereby optimize differentiation. We first investigated the integrin expression in both naive hMSCs and hMSCs undergoing osteogenic and adipogenic differentiation. To simplify the complex extracellular environment, we used a self-assembled maleimide-functionalized polystyrene-block-poly(ethylene oxide) copolymer (PS-PEO) surface [36] to present short (6–15mer) peptide sequences to hMSCs with known specificity for a limited number of integrin pairs. The cell-binding motifs presented were RGD, RRETAWA, IKVAV, and YIGSR. RGD is a widely occurring cell adhesion motif that is known to bind through integrins α5β1, α8β1, αVβ1, αIIbβ3, αVβ3, αVβ5, and αVβ6 [37,38], while RRETAWA is a synthetically derived sequence with specificity for only α5β1 [39]. IKVAV and YIGSR are both laminin-derived motifs; IKVAV is a binding domain from the laminin α1 chain, while YIGSR is derived from the β1 chain [40,41]. Both motifs are thought to be bound through combinations of α3β1, α4β1, and α6β1 integrins, although there are conflicting reports within literature [42–44]. This highly tailored surface was then used to determine how specific integrin–ligand interactions affect hMSC differentiation. This provides vital knowledge for the future development of biomaterials that present appropriate signals to achieve directed differentiation of hMSCs for tissue engineering applications.

Materials and Methods

All materials were purchased from Sigma unless otherwise stated. Peptides were ordered from Genscript.

hMSC culture and characterization

hMSCs were isolated from the bone marrow of healthy 18–60-year-old volunteers after obtaining written informed consent (MHS HREC number 740A, MMRI ethics number 32). Briefly, 10 mL of bone marrow aspirate taken from the iliac crest was resuspended in 20 mL phosphate-buffered saline (PBS) and the mononuclear fraction was separated by Percoll density gradient. The mononuclear cells were resuspended in low-glucose Dulbecco's modified Eagle's medium (DMEM) supplemented with penicillin/streptomycin (10,000 units; Gibco/Invitrogen) and 10% fetal bovine serum (FBS) and cultured in tissue culture flasks at 37°C in a humidified 5% CO_2 in air environment. After 24 h nonadherent cells were removed by exchanging the medium and the remaining cells were cultured with media changes every 3–4 days and passaging at 80% confluence. hMSCs at P4 were characterized by flow cytometry expressing surface markers CD29, CD44, CD49a, CD73, CD90, CD105, CD146, and CD166 and negative for CD34 and CD45. The cells displayed trilineage differentiation potential along the osteogenic, chondrogenic, and adipogenic lineages. hMSC characterization data can be found within a previous publication [45].

Differentiation

hMSCs were differentiated into the adipogenic and osteogenic lineages using standard differentiation protocols. For osteogenic differentiation, hMSCs were cultured in media containing 10% FBS, 100 $ng \cdot mL^{-1}$ dexamethasone, 50 μM ascorbate-2-phosphate, and 10 mM β-glycerophosphate in low-glucose DMEM, which was changed every 3–4 days. Differentiation was assessed via staining of alkaline phosphatase and calcium phosphate deposits (using Alizarin red) at 7, 14, and 21 days. For adipogenic differentiation, hMSCs were cultured in media containing 10% FBS, 1 $\mu g \cdot mL^{-1}$ dexamethasone, 0.2 mM indomethacin, 0.5 mM isobutyl-1-methylxanthine, and 10 $\mu g \cdot mL^{-1}$ insulin in DMEM, which was changed every 3–4 days. Differentiation was assessed via Oil Red O staining of the fatty vacuoles at 7, 14, and 21 days.

For integrin and ECM expression analysis, hMSCs were seeded at 1×10^4 cells per cm^2 and 2×10^4 cells per cm^2 for osteogenic and adipogenic differentiation, respectively (standard differentiation densities), while differentiation upon the PS-PEO substrates was performed at a density of 5×10^3 cells per cm^2 for both lineages.

Histological staining

After differentiation the extent of osteogenic differentiation was assessed by alkaline phosphatase and Alizarin red staining. To detect alkaline phosphatase activity hMSCs were washed with PBS and incubated in 1 mg·mL^{-1} Fast Red-TR and 0.2 mg mL^{-1} Napthol AS-MX Phosphate in 0.1 M Tris-HCl (pH 9.2) for 2 min at room temperature (RT). Cultures were then washed with dH_2O and fixed in 4% paraformaldehyde (PFA). Alizarin red staining was performed on hMSC cultures fixed for 10 min in 4% PFA. The cells were then washed thoroughly in dH_2O and stained with 2% Alizarin red (pH 4.2) for 30 min. Adipogenic differentiation was assessed by staining for 30 min using 60% Oil Red O in water (from a 0.5% Oil Red O in isopropanol stock).

Flow cytometric analysis of integrin subunit expression

Cells were detached from culture and then live, unfixed cells were stained for antibodies against α1 (clone-FB12), α2 (clone-P1E6), α3 (clone-P1B1), α4 (clone-P1H4), α5 (clone-P1D6), α6 (clone-NKIGoH3), and αV (clone-P3G8), and β1 (clone-MAR4), β2 (clone-P4H9), β3 (clone-25E11), β4 (clone-ASC-9), and β5 (clone-N/A) integrins {all from Millipore [α-integrin kit (ECM430) and β-integrin kit (ECM440)], except β1 integrin from BD Bioscience (555442)}. These were then visualized using appropriate secondary antibodies raised against mouse-IgG1, mouse-IgG2A, rat-IgG, and rabbit-IgG conjugated to Alexafluor 488 (all from Invitrogen). The samples were analyzed on an LSRII flow cytometer (B&D Biosciences) counting at least 10,000 cells per condition. Mature adipocytes were gated according to increased forward and side-scatter properties associated with an increase in both cell size and lipid vacuole formation (Supplementary Fig. S1A; Supplementary Data are available online at www.liebertonline.com/scd). The percentage of the cell population with positive expression was classified as that above 95% of the appropriate IgG control population. Representative histogram profiles are displayed in Supplementary Fig. S1B.

Cell morphology and ECM immunolocalization

hMSCs were fixed in 1% PFA for 10 min at room temperature followed by incubation in blocking buffer (3% bovine serum albumin in PBS) for 60 min. Cells were then stained with primary antibodies specific to fibronectin (1:400; Sigma-Aldrich), laminin (1:100), collagen-I (1:200), and collagen-IV (1:200; all from Abcam) or the relevant IgG control (Invitrogen) for 45 min at RT and with Alexa 488-conjugated secondary antibodies (Invitrogen and Abcam) for 30 min at RT. Cells were then permeabilized with 0.1% Triton X-100 and stained with Hoechst 33342 (1:2,000) and rhodamine-phalloidin (1:40) for 45 min at RT. Stained cells were imaged using an Olympus IX81 fluorescent microscope.

Preparation of block copolymer surfaces

PS-PEO copolymer with 51 kDa polystyrene (PS) block and 11.5 kDa PEO block (Polymer Source Pty. Ltd.) was maleimide functionalized as described previously [36]. This was made up as a 1% (w/v) solution in toluene (Sigma-Aldrich) and spin-coated onto glass coverslips. These surfaces were sterilized in 70% ethanol before incubation for 2 h with 20 μg·mL^{-1} peptide (CG**RGD**S, CGGG**RRETAWA**, CGQAAS**IKVAV**SADR, or CGGEGYGEG**YIGSR**) in 0.1 M sodium phosphate/0.15 M sodium chloride/10 mM ethylenediaminetetraacetic acid (pH 7.2). Surfaces were washed thoroughly in PBS prior to cell attachment.

Integrin-blocking assays

hMSCs were incubated with blocking antibodies to specific integrins α3, α4, α5, α6, and α8 [Abcam (ab56355)]; αV and αIIbβ3 [clone-PAC-1; BD Bioscience (340535)]; β1, β3, β5, and αVβ6 [clone-10D5; Millipore (MAB2077Z)] for 1 h prior to cell seeding (if antibody details are not stated, refer to those previously listed). Antibodies were used at a concentration of 10 μg·mL^{-1}, with the exception of α8 and β1 that were used at 5 μg·mL^{-1}. hMSCs were then seeded onto peptide surfaces at a density of 5,000 cells per cm^2 in serum-free media, with blocking antibodies still present, and allowed to attach for 2 h. To determine cell attachment levels, cells were washed twice in PBS and fixed for 20 min in 4% PFA (Sigma-Aldrich). Cells were stained with 0.1% (w/v) crystal violet (Sigma-Aldrich) in 200 mM 2-(*N*-morpholine) ethanesulfonic acid (Sigma-Aldrich) (pH 6.0) for 10 min and washed 5 times in ddH_2O to remove excess crystal violet before addition of 200 μL of 10% glacial acetic acid. Absorbance was read at 590 nm using a Spectramax M5 Fluorometer (Molecular Devices).

Quantitative real-time polymerase chain reaction

After 10 days of differentiation on the different peptide surfaces, total RNA was extracted using the RNeasy Minikit with on-column DNase treatment (Qiagen) according to the manufacturer's instructions. cDNA was synthesized using 100 ng RNA and 200 U SuperScript III, or the equivalent volume of DNase and RNase-free water for no-RT controls, in a total volume of 25 μL. qPCRs were set up in a total volume of 10 μL with 1×Platinum SYBR Green qPCR SuperMix-UDG (Invitrogen) and 0.2 μM forward and reverse primers (Table 1). A 7500 Fast Real-Time PCR System (Applied Biosystems) with fast cycling parameters of 2 min at 50°C, 2 min at 95°C, and then 40 cycles of 3 s at 95°C and 30 s at 60°C followed by a melt curve was used to run the samples. Data were analyzed using the $2^{-\Delta Ct}$ method using glyceraldehyde 3-phosphate dehydrogenase (GAPDH) as a reference gene. Levels of GAPDH were determined to be constant [statistically equivalent using analysis of variance (ANOVA) ($P = 0.4$–1)] across all conditions (Supplementary Fig. S2).

Results and Discussion

Naive hMSCs express a wide range of integrin subunits

Flow cytometry was used to determine the integrin expression profile of naive bone marrow–derived hMSCs from 4 independent donors. Over 80% of the population expressed

Table 1. Details of qPCR Primer Sequences

Gene	*Forward primer 5′-3′*	*Reverse primer 5′-3′*	*NCBI accession number*
GAPDH	ATGGGGAAGGTGAAGGTCG	TAAAAGCAGCCCTGGTGACC	
PPARγ	GGCTTCATGACAAGGGAGTTTC	AACTCAAACTTGGGCTCCATAAAG	NM_015869
LPL	GAGGTACTTTTCAGCCAGGATGTAAC	AGCTGGTCCACATCTCCAAGTC	BT006726
Runx2	AGTGATTTAGGGCGCATTCCT	GGAGGGCCGTGGGTTCT	NM001024630

α1, α3, αV, and β1 and β2 integrins, while α2, α4, and α5 were expressed by 40%–80% of hMSCs (Fig. 1). The lower mean expression of these can be attributed to large interdonor variability; 2 of the 4 donors expressed high levels of integrins α2 and α4 and 1 donor expressed high levels of α5 (Table 2). Less than 20% of the population expressed integrins α6, β3, β4, and β5.

Our study is consistent with others in showing that hMSCs express α1, α2, α5, αV, and β1 integrins, although we observe lower levels of α6 than is commonly reported [17,21,46]. We also observed significant expression of the α3 and β2 integrin subunits (β2 had the highest mean fluorescent intensity of all integrins; data not shown). These integrins have been previously reported to be expressed by hMSCs, although their observed expression is inconsistent between studies. α3 is expressed by whole plastic adherent hMSC populations, while it is not detected when examining Stro-1-selected hMSCs, and as such, expression may be a result of the starting population used [17]. Similarly, β2 expression has been previously described [47,48] but it is not ubiquitously reported. However, due to the alpha subunits that dimerize with β2 integrin (αD, αM, and αX), it is not likely to be a major mediator of ECM interactions but could be involved in cell–cell interactions [49]. We also observed a large amount of interdonor variability in the integrin subunits α4, β3, β4, and β5. This is consistent with a recent study by Semon et al. [48] that also observed significant hMSC donor–donor variability and could explain the contradictory expression levels previously reported for integrins α4, β3, and β4 [46,48,50].

hMSC integrin expression changes during osteogenic differentiation

We then investigated how integrin expression would change during hMSC differentiation along the osteo- and adipogenic lineages (chondrogenic differentiation has been well studied and so was not investigated [22,24,51,52]). Flow cytometry was used to determine the expression of our panel of integrin subunits after 7, 14, and 21 days of differentiation and lineage commitment was confirmed by alkaline phosphatase and Alizarin red staining for osteogenesis (Supplementary Fig. S3A, B) and Oil Red O staining for adipogenesis (Supplementary Fig. S3C).

During osteogenic differentiation we observed a significant, but transient, increase in integrin α5 on day 7, with the proportion of α5-positive cells increasing from 28% in naive MSCs to 99% and subsequently decreasing to 15% and 7% on days 14 and 21, respectively. There was also a significant reduction in the expression of integrins α1, α2, and α3 on day 21 of osteogenesis. In addition, a decreasing trend in the levels of α4, β3, and β4 subunits was observed, with expression reduced to <20% in all donors by day 21 (although due to variation in the level in the initial population these were not statistically significant) (Fig. 2; Supplementary Table S1).

The transient expression of α5 integrin that we observed is consistent with previous studies investigating MSC–osteoblast differentiation [26,34,53]. It has also been suggested that integrins α2β1 and αvβ3 increase transiently at day 7 of osteogenesis, decreasing to basal levels by day 14 [53]. However, in contrast to integrin α5, we did not observe a peak in the expression of these subunits. Instead we observed a reduction in α2, αV, and β3 expression on day 14 compared with initial levels (although donor variability meant that these changes were not statistically significant). We hypothesize that these and other changes in integrin expression may be due to time in culture and confluence because the

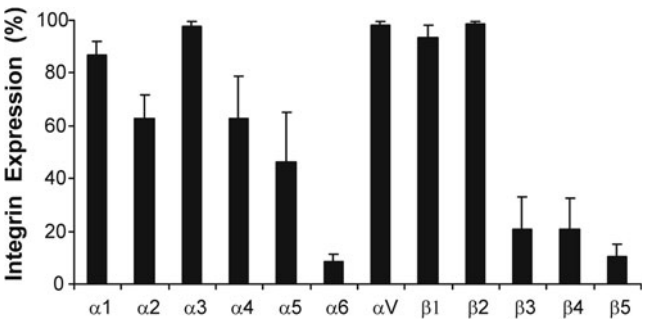

FIG. 1. Integrin expression profile of bone marrow–derived hMSCs. The mean percentage of the hMSC population expressing each integrin subunit is shown (±SD) for hMSCs from 4 independent donors. MSCs, mesenchymal stem cells; hMSCs, human bone marrow–derived MSCs; SD, standard deviation.

Table 2. Integrin Expression by Bone Marrow–Derived Mesenchymal Stem Cells

	Percentage expression					
Integrin	*Donor 1*	*Donor 2*	*Donor 3*	*Donor 4*	*Mean*	*SD*
α1	87.9	71	91.5	95.9	86.6	10.9
α2	72.2	46.2	51.2	82.2	63.0	17.1
α3	100	97.6	100	92.7	97.6	3.4
α4	89.9	20	58	83.1	62.8	31.6
α5	99.9	14.1	36.1	35.2	46.3	37.1
α6	15.9	4.89	5.39	8.33	8.6	5.1
αV	99.8	92.9	99.4	99.8	98.0	3.4
β1	79	96.6	99.4	98.6	93.4	9.7
β2	99.6	95.4	99.1	99.9	98.5	2.1
β3	8.62	8.47	7.75	57.9	20.7	24.8
β4	12.7	7.44	7.28	56.2	20.9	23.7
β5	24.7	5.74	7.56	3.66	10.4	9.7

The percentage of the population expressing each integrin subunit for hMSCs from 4 independent donors is presented in the table.
SD, standard deviation.

decrease in α2, α3, α4, β3, and β4 expression under osteogenic conditions was mirrored within cultures expanded for 21 days under control conditions (Supplementary Fig. S4). Changes in integrin expression in response to confluency have also been suggested in previous studies [48].

hMSC integrin expression changes during adipogenic differentiation

For adipogenic differentiation we observed a significantly increased proportion of α6-positive hMSCs after 21 days of differentiation as well as a significant reduction in α2 and α4 integrins after 14 and 21 days and in α3 integrin after 21 days (Fig. 3; Supplementary Table S2). Similar to osteogenesis, there was again a decreasing trend in the levels of α4, β3, and β4 subunits for those donors in which there were substantial levels in the undifferentiated population.

The increase in expression of α6 integrin correlates with Liu et al. [27] who described a switch from α5 to α6 integrin expression during differentiation of 3T3-L1 preadipocytes, although we are the first to report the changes in integrin expression during adipogenic differentiation of primary hMSCs. Our results differ in that we do not observe a significant decrease in α5 expression. The reduced expression of α2, α3, α4, β3, and β4 is similar to decreases seen within osteogenesis and under control conditions. This further supports our hypothesis that expression of these integrin subunits changes as a result of time in culture and prolonged confluence.

Deposition of collagen-I and collagen-IV increases during osteogenesis

To investigate how changes in integrin expression may correlate with any changes in the ECM that the integrins bind to, we used immunocytochemistry to examine both the expression levels and organization of collagen-I, collagen-IV, fibronectin, and laminin during differentiation.

During osteogenesis, levels of collagen-I and collagen-IV increased. This collagen was initially in the form of fibrillar strands but was reorganized to a diffuse, less-defined globular pattern by days 14 and 21. Fibronectin levels decreased as the hMSCs both underwent osteogenesis and were sustained in culture although this degradation was more prominent within the differentiation conditions. This was organized as strands that aligned predominately with actin filaments. No laminin was detected in any of the cultures (Fig. 4).

This data is consistent with previous reports that collagen-I synthesis increases during MSC to osteoblast differentiation [53,54] as well as the high expression reported for human osteoblasts [55,56]. Fibronectin has been shown to be expressed throughout osteogenesis with levels remaining relatively unchanged in both control and osteogenic conditions [53,54], which differs from the decreased expression we

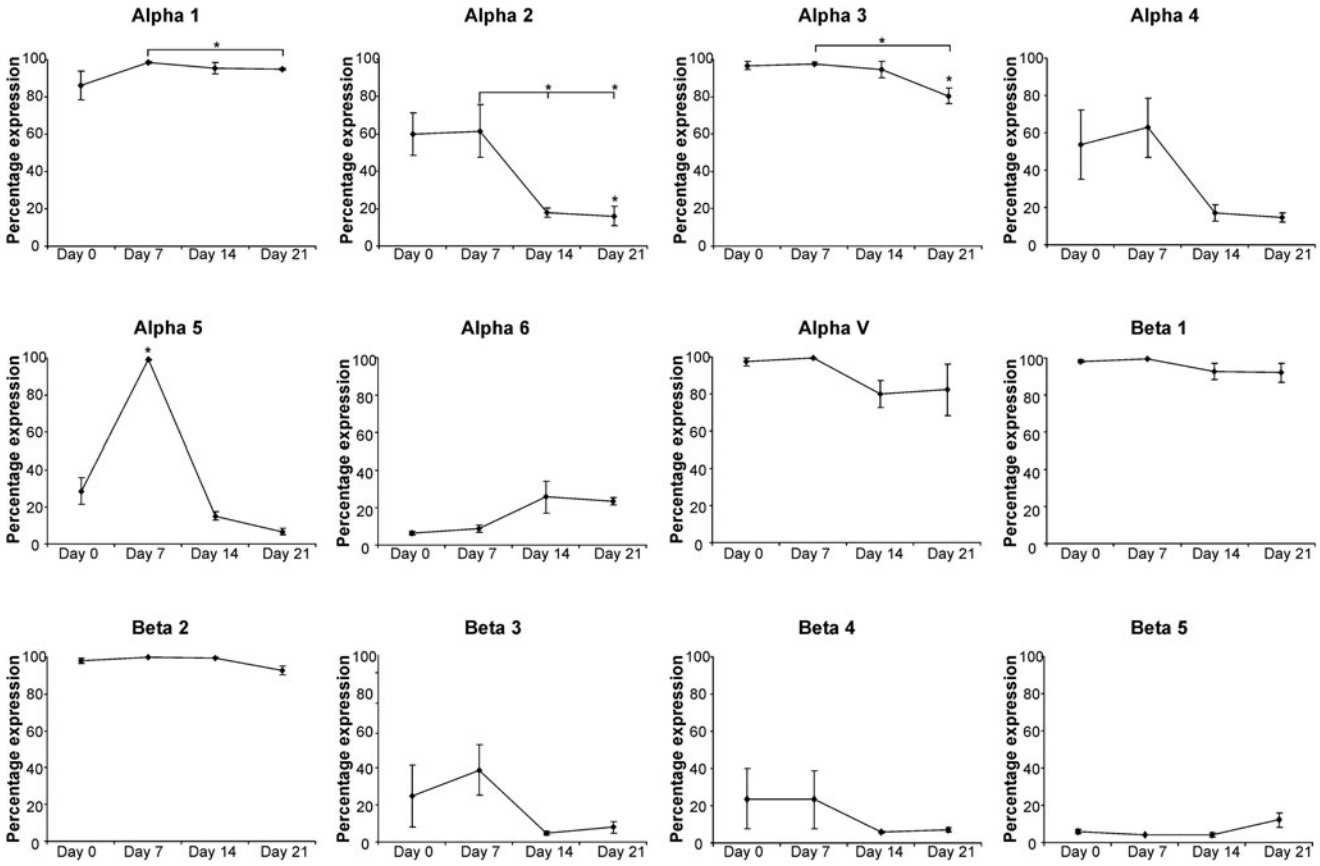

FIG. 2. Integrin expression in hMSCs throughout osteogenic differentiation. The mean percentage of the hMSC population expressing each integrin subunit is shown (±SD) for hMSCs from 3 independent donors after 7, 14, and 21 days of osteogenic differentiation. Statistical significance was determined by one-way analysis of variance (ANOVA); $*P < 0.05$.

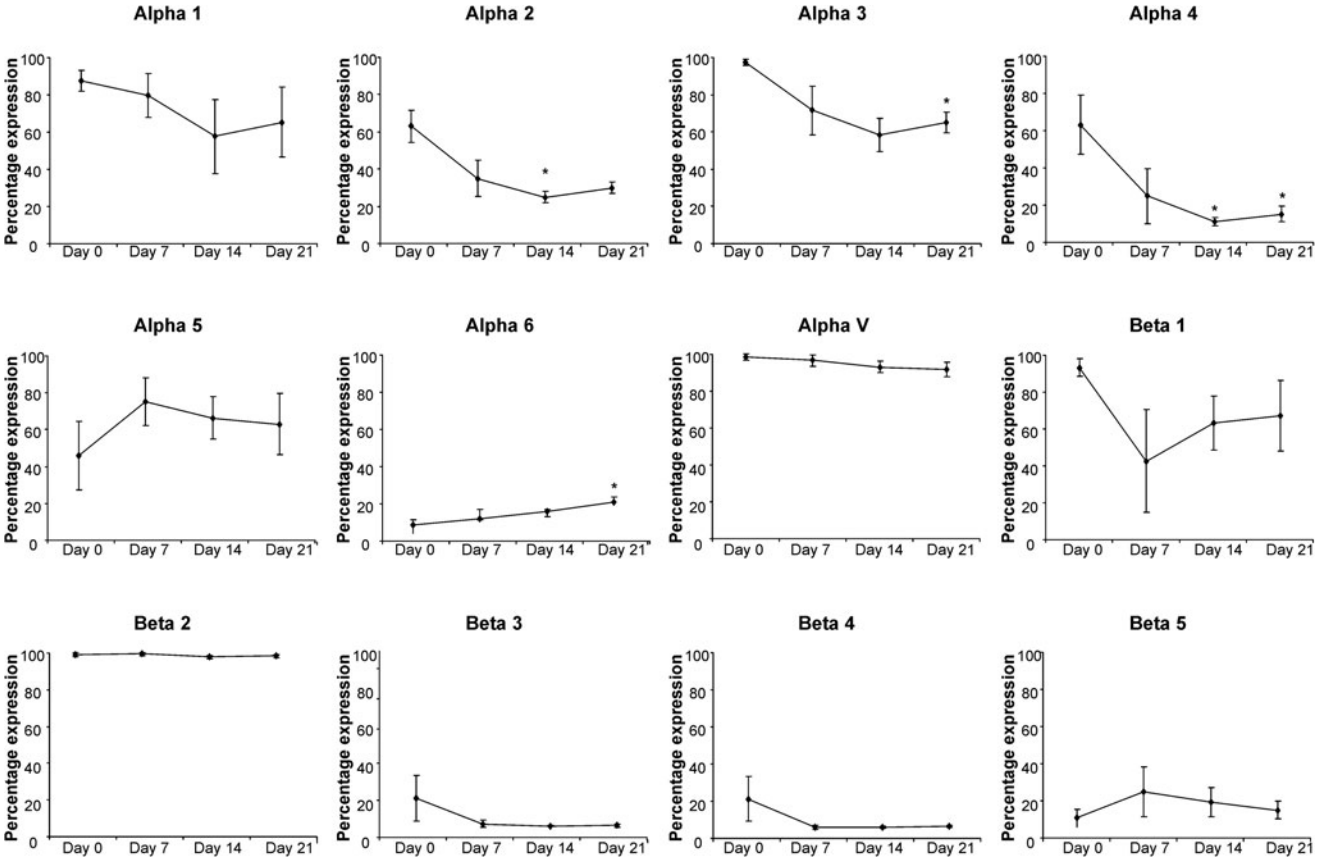

FIG. 3. Integrin expression in hMSCs throughout adipogenic differentiation. The mean percentage of the hMSC population expressing each integrin subunit is shown (±SD) for hMSCs from 4 independent donors after 7, 14, and 21 days of adipogenic differentiation. Statistical significance was determined by one-way ANOVA; $*P < 0.05$.

observed at the end stage of differentiation. The highly aligned arrangement of fibronectin we observed also differs to that seen by Kundu et al. [53a], who described a disorganized fibronectin arrangement. However, our data more closely matches with the fibronectin deposited by human osteoblasts cultured in vitro [57].

Laminin deposition increases with adipogenic differentiation

During adipogenesis there was an increase in the level of collagen-I, collagen-IV, and laminin, with notable deposition of collagen-IV and laminin by day 14 and of collagen-I by day 21 (Fig. 5). The laminin was organized as punctuate dots, and by overlaying phase-contrast images with immunofluorescence, it was clear that the laminin was distributed primarily around those cells with well-developed fat vacuoles (Fig. 5, inset). Similar to osteogenesis, the structure of the deposited collagens changed from fibrillar strands to a more globular structure. Fibronectin was also remodeled in the adipogenic cultures to a less diffuse, globular arrangement by day 14 and was completely absent by day 21. This contrasted with the progressive increase in fibronectin deposition seen in undifferentiated cultures.

There are no previous reports of the changes to ECM expression and arrangement as hMSCs undergo adipogenesis. However, our data is consistent with studies using preadipocyte cell lines that show an increased collagen-I, collagen-IV, and laminin expression and a degradation of fibronectin [58–60]. Integrin α6 is a known laminin-binding integrin and so the increased laminin that we observe during adipogenesis correlates with the increase in α6 expression and has also been shown to control the migration and aggregation of adipocytes on laminin substrates [27].

hMSCs adhere to peptide motifs via specific integrin pairs

To probe explicit integrin–ECM interactions and how these influence hMSC behavior and differentiation potential, we used a PS-PEO copolymer surface [36,61] as a platform with which to present ECM-mimetic peptides with known integrin specificity to hMSCs (Fig. 6A, B). This substrate consists of a microphase-separated surface of separate, vertically oriented PEO cylinders within a background of PS polymer. The cell adhesion peptides are tethered to the PEO chains thereby producing a substrate upon which short specific sequences are presented to the cells in a geospatially controlled manner. The motifs presented were the fibronectin-derived RGD, the laminin-derived IKVAV and YIGSR sequences, and RRETAWA, a synthetic sequence with specificity for α5β1 integrin [39].

To confirm integrin-peptide specificity, hMSCs were treated with integrin-blocking antibodies and their adhesion to each of the different peptide motifs was assessed. Attachment to RGD was significantly diminished when

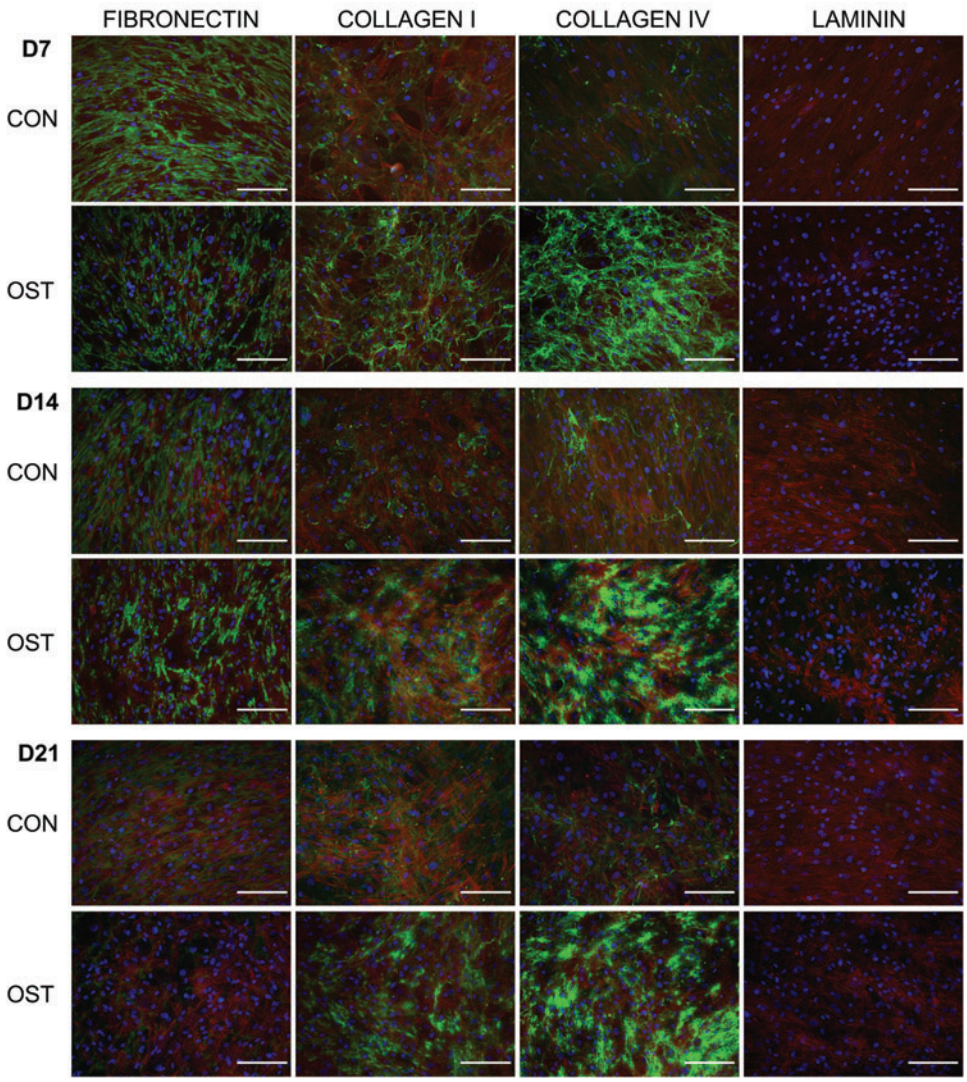

FIG. 4. Immunolocalization of ECM components during osteogenic differentiation. Immunofluorescent staining of hMSCs for fibronectin, collagen-I, collagen-IV, and laminin after 7, 14, and 21 days of osteogenic differentiation showing ECM components (*green*), actin (*red*), and nuclei (*blue*). Scale bars represent 200 μm. ECM, extracellular matrix. Color images available online at www.liebertonline.com/scd

integrins α5β1, αVβ1, αVβ3, αVβ5, and αVβ6 were blocked, with adhesion completely abolished when all known RGD ligating integrins were blocked together (Fig. 6C). This was equivalent to surfaces functionalized with a cryptic RGD peptide, which also showed no cell adhesion. This demonstrates that hMSC adhesion to the PS-PEO surfaces was mediated through the RGD peptide and more specifically through the explicit interactions of the integrin subunits α5, αV, β1, β3, β5, and β6. Binding to RGD has been reported for multiple integrin subunits, of which the majority of binding is known to be facilitated by α5β1, αVβ3, and αVβ5 [38,39,62]. This correlates well with our data, as these integrin subunits, in addition to αVβ1, were responsible for the majority of adhesion (~80%). Adhesion to the α5β1-specific RRETAWA motif [39] was significantly reduced, to approximately 10% of that of the isotype control, in the presence of antibodies directed against α5β1, but not by antibodies that blocked αVβ3, thus confirming specificity of binding to the α5β1 sequence (Fig. 6D). IKVAV and YIGSR sequences are known to be bound by integrins α3β1, α4β1, and α6β1 [42,43]. We found that adhesion to both sequences was significantly diminished in the presence of both α4- and α6β1-blocking antibodies but was not affected when blocking α3β1. There was also a significant reduction in hMSC adhesion to YIGSR when blocking integrins α4β1 and α6β1 individually; however, adhesion to IKVAV was only significantly reduced when blocking α4β1 (α6β1, *P*-value = 0.06) (Fig. 6E, F), showing some differences in the specificity for the 2 different laminin-derived sequences. In some cases there was some residual binding of hMSCs to the PS-PEO surfaces (between 10% and 30% of isotype control). It is likely that this is due to incomplete antibody blocking and integrin recycling because, even in the presence of serum, hMSCs could not adhere to nonfunctionalized PS-PEO surfaces (Fig. 8D). This supports previous work in our laboratory on the nonfouling nature of this surface [61] and the specificity of the interaction of the hMSCs to peptides presented on the PS-PEO surfaces. This system thus provided an ideal platform with which to further probe the effect of integrin–ECM interactions on hMSC differentiation.

hMSC morphology is affected by different ECM motifs

Due to the central role of integrin binding in cell adhesion and spreading through focal adhesion assembly and

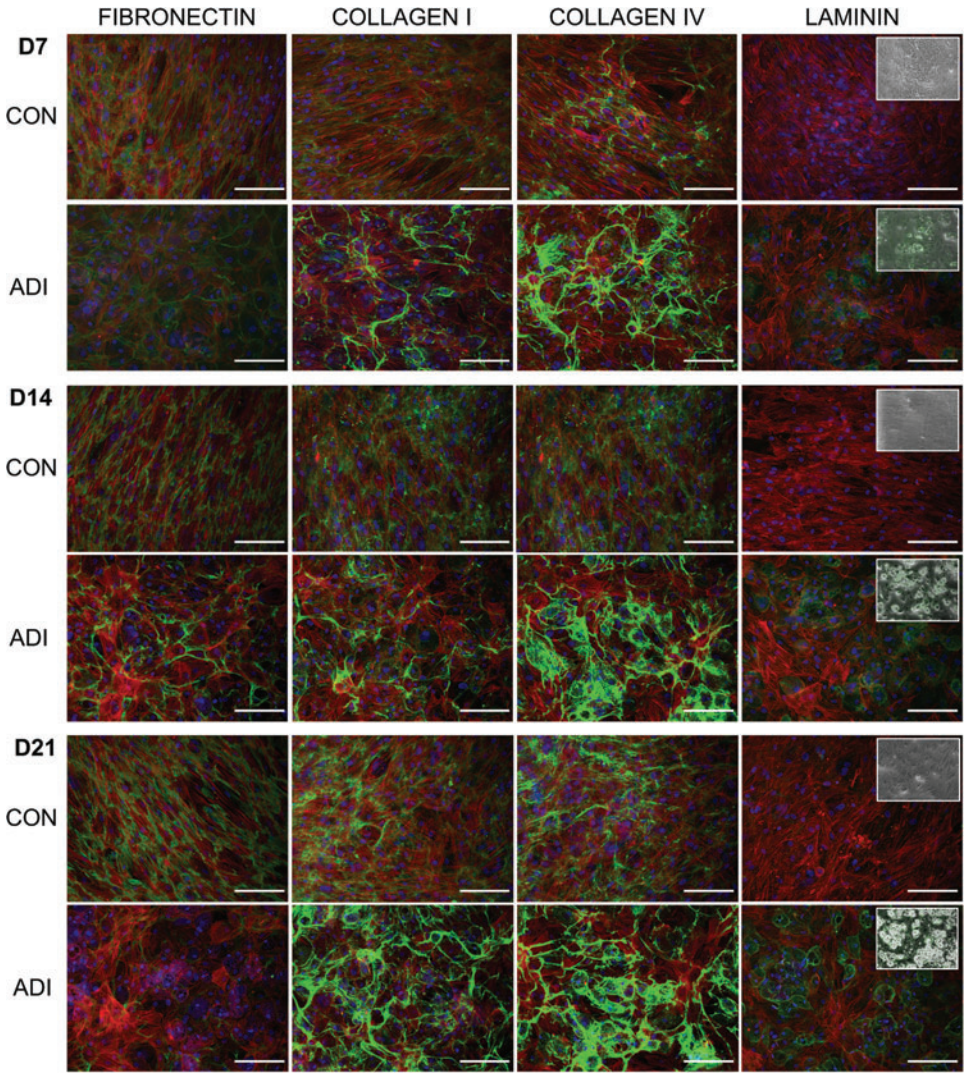

FIG. 5. Immunolocalization of ECM components during adipogenic differentiation. Immunofluorescent staining of hMSCs for fibronectin, collagen-I, collagen-IV, and laminin after 7, 14, and 21 days of adipogenic differentiation showing ECM components (*green*), actin (*red*), and nuclei (*blue*). Scale bars represent 200 μm. *Insets* show phase-contrast images overlaid with laminin expression. Color images available online at www.liebertonline.com/scd

cytoskeletal remodeling, we first investigated the effect of the different peptide motifs on hMSC morphology. hMSCs were seeded (under serum-free conditions) onto surfaces presenting each of the peptides and their morphology was assessed after 24 h. hMSCs had the greatest ability to spread on substrates presenting RGD peptide, displaying a classic fibroblastic morphology. Some spreading was also observed on RRETAWA, although the morphology of these hMSCs was somewhat different, with cells extending 3–4 broad filopodia. On both IKVAV and YIGSR, the hMSCs did not spread and remained rounded, although those on YIGSR showed some membrane protrusion around the cell periphery (Fig. 7A). Closer analysis of the cytoskeleton showed that hMSCs on RGD had prominent stress fibers running through the cell body with distinct focal adhesions localized at their ends. These stress fibers were also evident in hMSCs on RRETAWA, although these were arranged around the periphery of the cell. Neither hMSCs on IKVAV or YIGSR developed stress fibers, instead presented a disorganized actin cytoskeleton mainly localized at the cell periphery. Consistent with the lack of stress fiber development, no mature focal adhesions were detected in hMSCs on RRETAWA, IKVAV, or YIGSR (Fig. 7B).

The greatest amount of spreading was observed on the RGD peptide, which is bound by α5β1, α8β1, αVβ1, αIIbβ3, αVβ3, αVβ5, and αVβ6 integrins. A study by Roca-Cusachs et al. [53] determined that the integrins α5β1 and αVβ3 have different functions, with α5β1 determining adhesion strength while αVβ3 mediated mechanotransduction [65]. The differences in spreading and cell morphology observed between hMSCs on RGD and RRETAWA (which is only bound by α5β1) may therefore suggest that both of these functions need to be fulfilled for effective cell spreading and cytoskeletal organization. In addition, RGD and RRETAWA were the only peptides on which hMSCs could form stress fibers. This suggests that the adhesions formed with α5β1 and not α4β1 or α6β1 integrin (as is the case on IKVAV and YIGSR) are required for stress fiber assembly. Overall, these observations demonstrate that engagement of different integrins can profoundly influence hMSC spreading, shape, and cytoskeletal organization.

hMSC survival on different ECM motifs

When initial differentiation studies were conducted we found that RRETAWA, IKVAV, or YIGSR alone could only

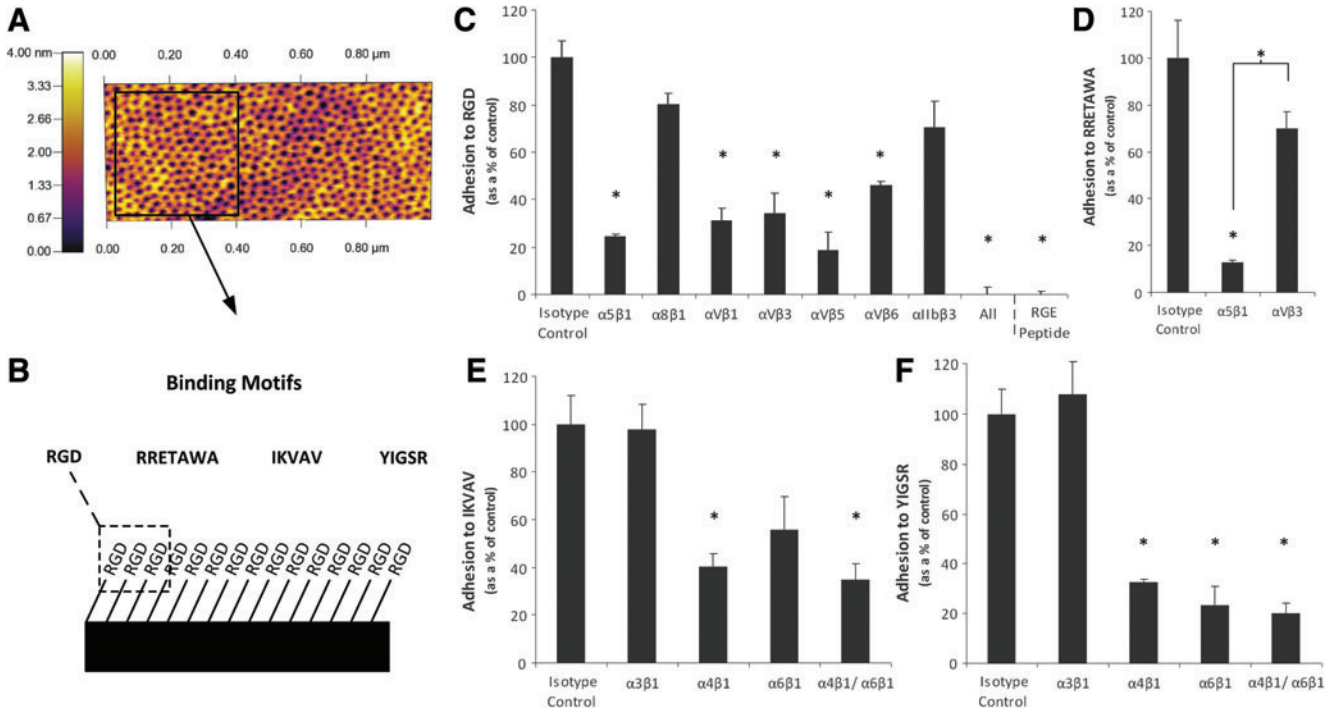

FIG. 6. Adhesion of hMSCs to specific peptides presented on defined PS-PEO surfaces. Atomic force microscopy (AFM) image of a PS-PEO surface showing a background of PS with nanoislands of PEO to which adhesion peptides were bound **(A)**. Schematic representation of the PS-PEO surfaces presenting short peptide sequences with specificity for different integrins **(B)**. Integrin blocking of hMSC adhesion PS-PEO surfaces functionalized with **(C)** RGD, **(D)** RRETAWA, **(E)** IKVAV, and **(F)** YIGSR peptides. Adhesion is presented as mean percentage relative to isotype control treated hMSCs on PS-PEO surfaces for $n=3$. Statistical significance was determined by one-way ANOVA, $^*P<0.05$, relative to cells only. PS-PEO, polystyrene-block-poly(ethylene oxide) block copolymer; PS, polystyrene. Color images available online at www.liebertonline.com/scd

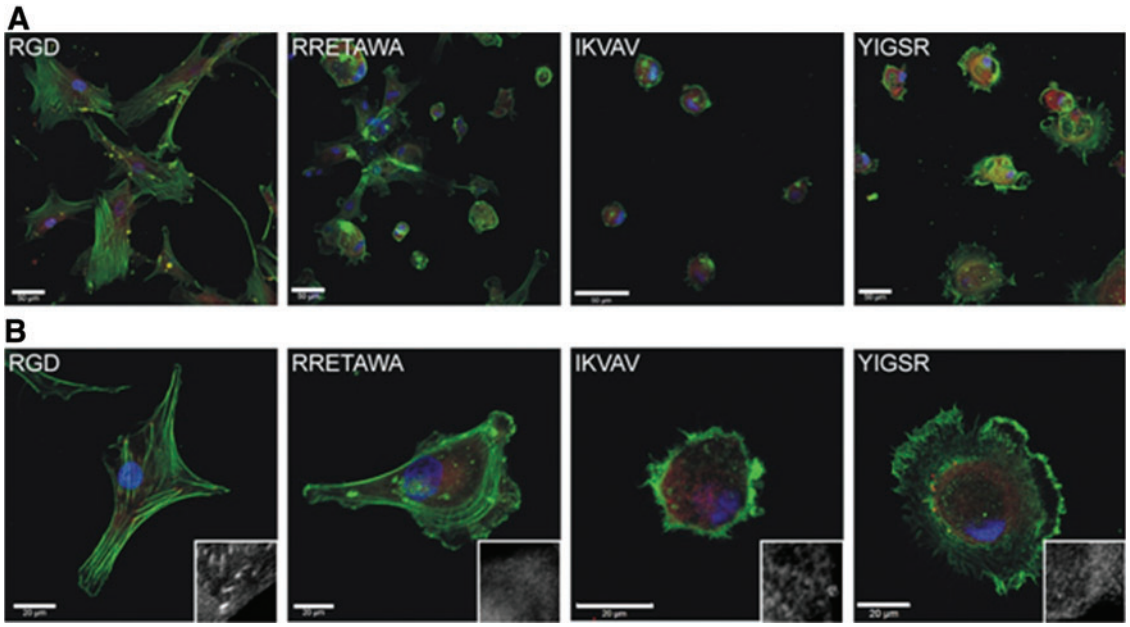

FIG. 7. hMSC morphology on different peptide motifs. Staining showing actin (*green*), focal adhesion (vinculin; *red*), and nuclei (*blue*) of hMSCs after 24 h on PS-PEO surfaces presenting different ECM motifs. Scale bars = 50 μm **(A)** and 50 μm **(B)**. *Insets* show the vinculin staining alone. Color images available online at www.liebertonline.com/scd

support hMSCs, in terms of attachment and viability, for periods shorter than 48 h (Supplementary Fig. S5A). To extend hMSC viability for the prolonged timescales required to determine differentiation potential, RGD peptide was added to surfaces presenting RRETAWA, IKVAV, or YIGSR peptides, over the range of 20%–1% RGD. Previous studies by our group have determined that when using molecules of a similar size, as is the case with the peptides used here, the attachment to the surface is homogenous and comparable to the ratio of ligand in solution [66]. The minimum level of RGD required to maintain hMSC attachment and viability for longer-term studies was 10% (Fig. 8C; Supplementary Fig. S5). The use of these substrates provided good adhesion across all peptides and allowed hMSCs to spread to a greater extent than seen on IKVAV or YIGSR alone, although differences in cell morphology were still visible between the different surfaces (Fig. 8A, B), indicating that the cells were responding to the major peptide presented on each surface.

ECM motifs influence osteogenic differentiation of hMSCs

hMSCs were seeded onto the different peptides and allowed to adhere in the absence of serum for 4 h. After this time the culture medium was replaced with medium containing osteogenic supplements [including FBS, although control cultures showed no attachment of hMSCs to blank PS-PEO substrates in the presence of FBS at any time up to 7 days (Fig. 8D)]. After 10 days of differentiation the relative expression of *Runx2* was significantly higher in hMSCs cultured on IKVAV surfaces compared with either RETTAWA or YIGSR (Fig. 9A). There were no significant differences in expression between hMSCs cultured on the other peptides. This correlated well with alkaline phosphatase staining, which showed increased activity in all differentiated cultures compared with the undifferentiated controls and particularly intense staining for hMSCs cultured on surfaces presenting IKVAV (Fig. 9B).

These results are unexpected, as we hypothesized that RRETAWA, which is specific for α5β1 integrin, would be the optimum peptide to promote osteogenesis. This is based on our data showing that α5 expression increases dramatically after 7 days of differentiation, as well as evidence that increasing the level of α5 via lentiviral overexpression enhances osteogenesis [26]. In addition, priming α5 with activating antibodies or soluble RRETAWA increased osteogenesis [26]. One explanation for this discrepancy may be that the hMSCs in the study by Hamidouche et al. [26] were firstly attached to tissue culture plastic and then treated with RRETAWA and so several integrins may have been activated due the adhesion of the cells to FBS adsorbed to the culture surface, in addition to the priming of α5 with the soluble peptide. This is very different to our defined surface in which

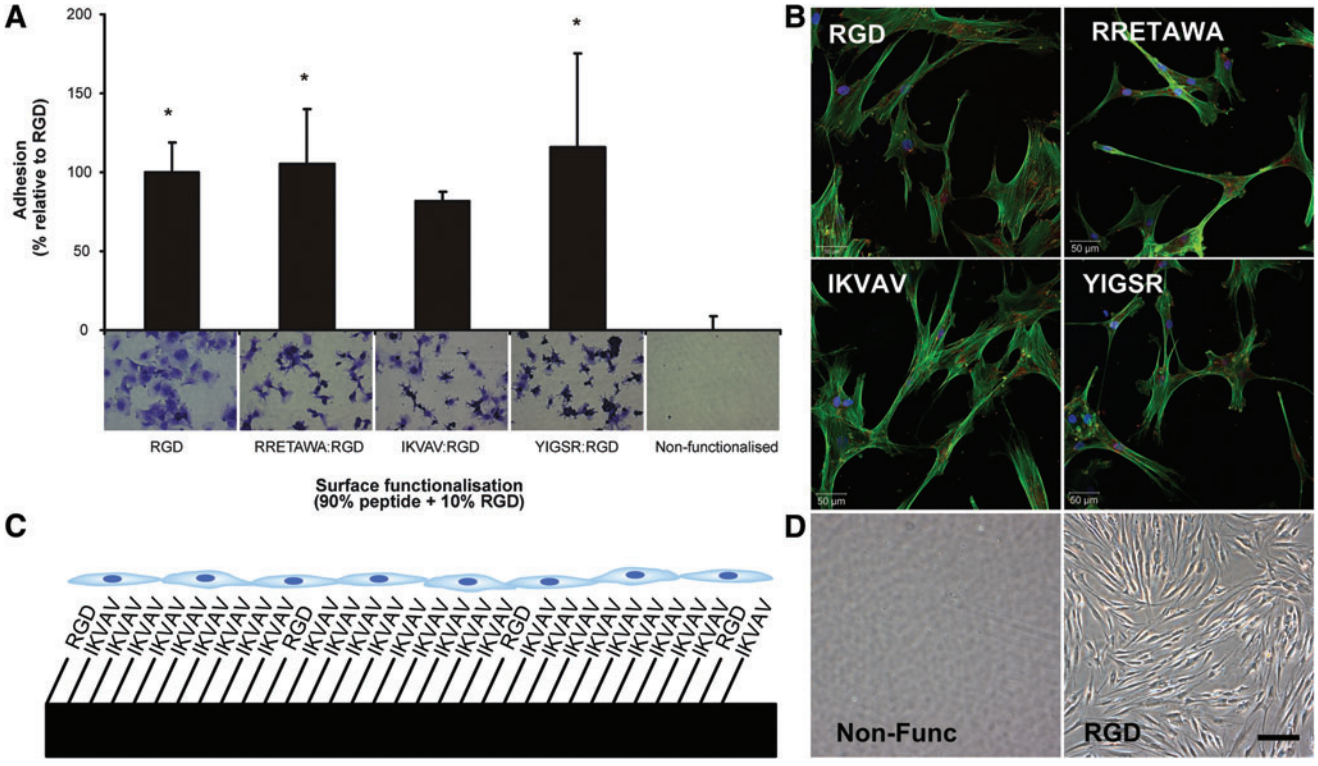

FIG. 8. Attachment and morphology of hMSCs on PS-PEO surfaces presenting peptides together with 10% RGD. **(A)** Adhesion of hMSCs to the peptide surfaces, presented as mean percentage relative to RGD-functionalized surfaces, $n = 3$. Statistical significance was determined by one-way ANOVA, $^*P < 0.05$, as compared with adhesion to the nonfunctionalized surfaces. **(B)** hMSC morphology on PS-PEO surfaces presenting different peptide motifs with 10% RGD. Staining shows actin (*green*), focal adhesion (vinculin; *red*), and nuclei (*blue*) of hMSCs after 24 h. **(C)** Schematic arrangement of the 10%–90% peptide surface functionalization. **(D)** Photomicrographs of hMSCs on an uncoated and RGD-functionalized PS-PEO surfaces after 1 week of culture in standard culture medium (low glucose Dulbecco's modified Eagle medium [LG-DMEM] plus 10% fetal bovine serum). Color images available online at www.liebertonline.com/scd

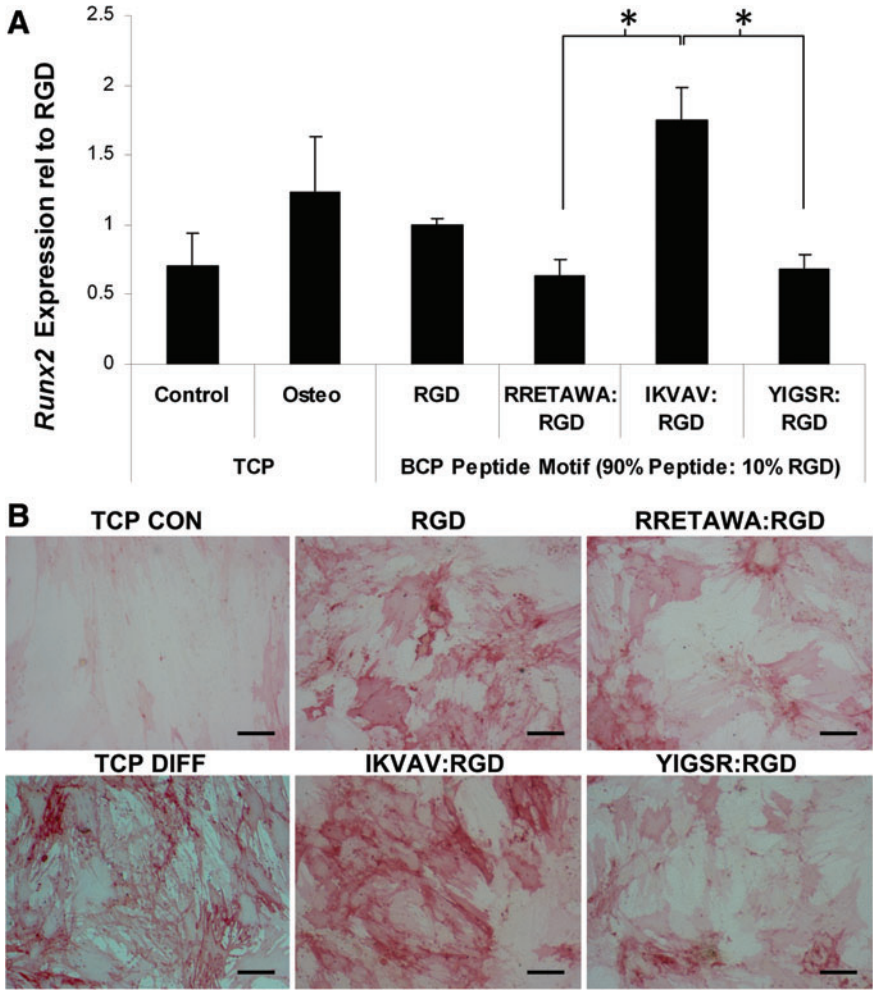

FIG. 9. Osteogenesis of hMSCs on different peptide motifs. qPCR determination of the relative expression of *Runx2* **(A)** in hMSCs differentiated for 10 days on different peptide surfaces. Data is presented as mean ± SEM, $n > 6$. Statistical significance was determined by one-way ANOVA; $^*P < 0.05$. **(B)** Alkaline phosphatase staining of osteogenic hMSCs. Scale bar = 100 μm. SEM, standard error of mean. Color images available online at www.liebertonline.com/scd

only the α5-specific peptide RRETAWA (and the small proportion of RGD that is bound predominately by α5β1, αVβ1, αVβ3, αVβ5, and αVβ6) would be available for integrin binding. This may also explain why the best surface for osteogenesis was that presenting IKVAV, as this surface has potential for activating integrins α4β1 and α6β1, as well as α5β1, αVβ1, αVβ3, αVβ5, and αVβ6 bound by the RGD component, providing a much broader range of integrin activation than the RRETAWA-functionalized surfaces, or those presenting RGD only.

It is clear from previous studies that a number of different ECM molecules can support osteogenesis, with hMSCs cultured on laminin-5, collagen-I, and vitronectin showing increased differentiation (in comparison to tissue culture plastic [TCP]) through interactions that were primarily mediated by integrins α3 and α6 for laminin-5 and α2β1 or αVβ3 for collagen-I and vitronectin, respectively [18,31]. Although these demonstrate that differentiation can be facilitated by the binding of a number of integrin subunits (in a way that is thought to involve signaling through a common mechanism involving FAK and ERK [18,26,29,30,67]), the complexity of the ECM molecules means that the effects of the individual integrin–matrix interactions could not be completely resolved. The ability to present a defined surface displaying specific, short peptide sequences that are only bound by 1 or 2 integrins allows us to see, for the first time, that recruitment of a wider range of integrins seems to be required for efficient differentiation to occur. Together with the fact that the situation is not as predictable as using the observed increase in α5 expression to enhance osteogenesis via a peptide specific for α5β1 integrin, this highlights the value of a defined platform, such as the PS-PEO surface, in elucidating the effects of such interactions on hMSC fate.

ECM motifs influence adipogenic differentiation of hMSCs

We next investigated whether the activation of different integrins via presentation of these ECM motifs, and the subsequent induced changes in cell morphology and cytoskeletal organization, would influence adipogenesis. The PS-PEO surfaces were used to present specific peptide motifs to hMSCs in conjunction with adipogenic supplements. After 10 days of differentiation the relative expression of peroxisome proliferator-activated receptor gamma (*PPARγ*) and lipoprotein lipase (*LPL*) was significantly higher in all adipogenic cultures compared with the TCP control condition, indicating that differentiation had occurred on all surfaces (Fig. 10A, B). IKVAV was once again found to be the most conducive surface for differentiation. While there was no significant difference in *PPARγ* expression between the different conditions, there was significantly higher expression

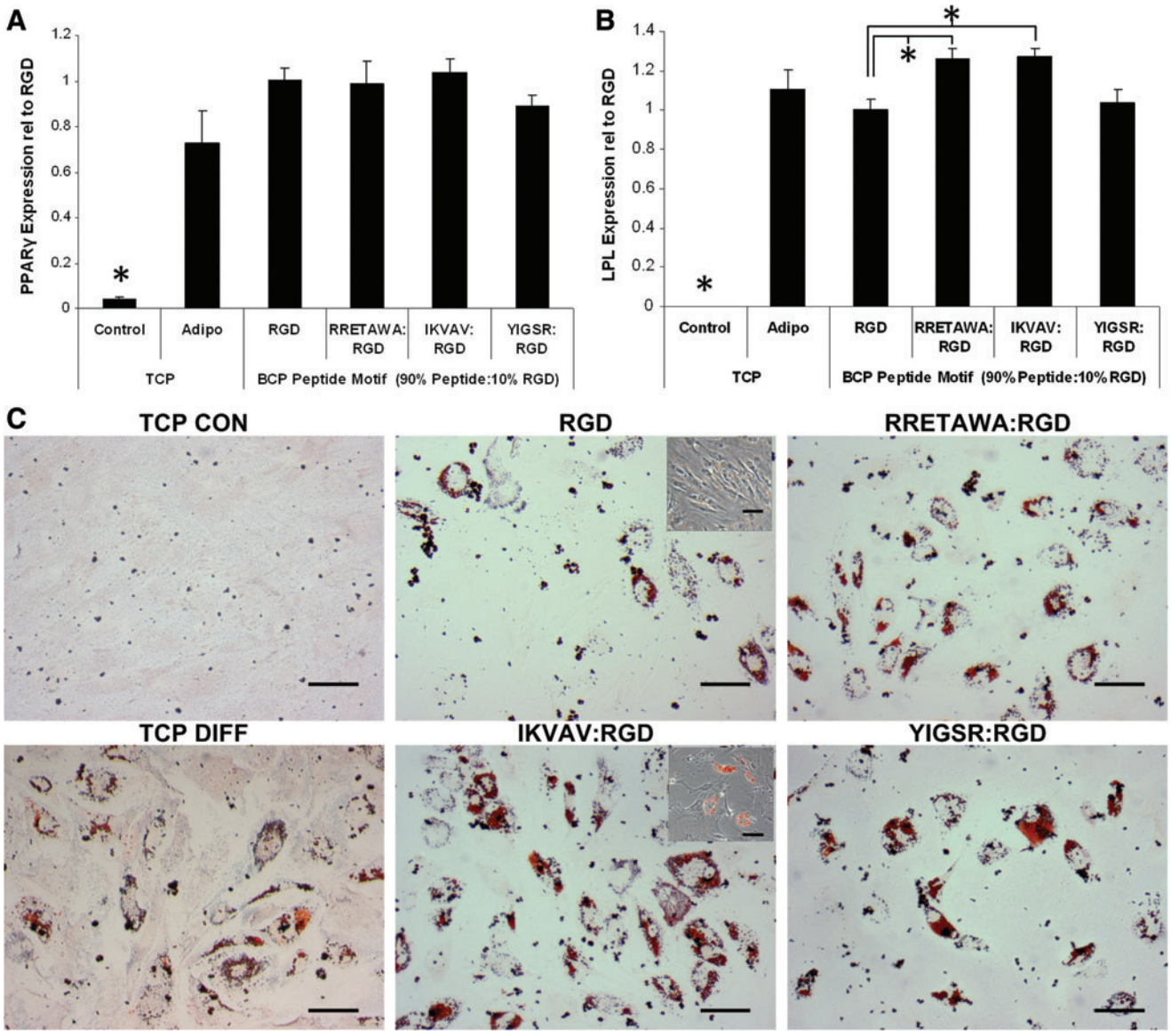

FIG. 10. Adipogenesis of hMSCs on different peptide motifs. qPCR determination of the relative expression of **(A)** *PPARγ* and LPL **(B)** in hMSCs differentiated for 10 days on different peptide surfaces. Data is presented as mean ± SEM, $n = 6$. Statistical significance was determined by one-way ANOVA; $^*P < 0.05$. **(C)** Oil Red O staining of adipogenic hMSCs. Scale bar = 100 μm. Color images available online at www.liebertonline.com/scd

of *LPL* in hMSCs on IKVAV and RRETAWA surfaces as compared with RGD. This was also reflected in the Oil Red O staining, with hMSCs on IKVAV displaying the greatest amount of fat vacuoles, followed by RRETAWA and YIGSR, with the least on RGD (Fig. 10C). Interestingly, it was observed that hMSCs on RGD retained the typical spindle morphology, in contrast to the large rounded morphology adapted by all of the other conditions (Fig. 10C, inset).

Although the effects of ECM on adipogenesis in hMSCs are unreported, the increased differentiation that we observe on PS-PEO surfaces presenting IKVAV corresponds well with our earlier data showing that expression of both laminin and integrin α6 (which binds to laminin) is increased during adipogenesis. It is again interesting to note the different outcomes for hMSCs on the laminin-derived peptides IKVAV and YIGSR, which further suggests functional differences in the downstream signaling affected by integrin binding to each of these motifs. The enhanced differentiation on IKVAV, compared with the fibronectin-derived RGD motif, also correlates with work on preadipocyte cell lines showing that laminin promoted adipogenesis [68], while fibronectin leads to the inhibition of differentiation by halting the necessary morphological changes (i.e., rounding up) [69,70]. This may indicate that the degradation of fibronectin that we observed in our analysis of ECM is necessary for successful progression down the adipogenic lineage. However, it is also important to note that it was necessary to functionalize the PS-PEO surface with 10% RGD peptide in addition to the 90% IKVAV in order to facilitate cell survival for the duration of the differentiation period. As such, in addition to the activation/recruitment of α4β1 and α6β1 integrins via the IKVAV sequence, integrins α5β1, α8β1, αVβ1,

αIIaβ3, αVβ3, αVβ5, and αVβ6 would also be bound (although in a lower proportion) to the RGD sequence. Overall, this activation of a broad range of integrins, as compared with the activation of a restricted range on RGD alone, may partly account for the increased differentiation of hMSCs on IKVAV surfaces as compared with RGD surfaces. Taken together, these results demonstrate that there are key morphological changes required for adipogenesis and the integrin–ECM interactions can enhance or inhibit the degree of differentiation.

Conclusion

This study provides the first comprehensive analysis of changes in integrin expression throughout differentiation of hMSCs, showing that osteogenesis is characterized by a sharp increase in integrin α5 expression at 7 days of differentiation, while adipogenesis can be marked by a significant increase in α6 expression. Alongside these changes in integrin expression, we observed increased collagen-I and collagen-IV and decreased fibronectin production during osteogenesis. Collagen-I and collagen-IV were also laid down during adipogenesis but with an additional substantial secretion of laminin. We used PS-PEO surfaces as a defined substrate upon which to present short peptides of known integrin specificity and investigate the hypothesis that differentiation could be optimized by activating α5 or α6 integrin for osteo- or adipogenesis, respectively. hMSCs cultured on PS-PEO surfaces displaying these peptides showed distinct morphologies, clearly demonstrating that different integrins have different functions. Surprisingly, our data showed that presenting a specific peptide to ligate integrin α5 did not provide the best conditions for osteogenesis, with the greatest amount of both osteo- and adipogenic induction on PS-PEO surface displaying the laminin-derived peptide IKVAV. Overall, this demonstrates that the lineage progression of hMSCs is influenced by the presentation of integrin-binding motifs, further confirming the role of integrin specificity in hMSC differentiation. Further, the ability to display short peptide sequences allows a level of specificity that has not previously been achieved through the use of protein domains or whole ECM molecules. This platform not only provides novel insight into hMSC–substrate interactions, but will also provide vital information for the future development of biomaterials capable of enhanced control of cell behavior for use in tissue engineering therapies.

Acknowledgments

The authors would like to acknowledge Dr. Gary Brooke (formerly of the Mater Medical Research Institute [MMRI], Brisbane, Australia) for initially isolating and expanding the hMSCs. Finally, the authors would like to acknowledge the financial support of the Australian Research Council Discovery Grants Scheme (DP0986619 and DP1095429), Australian Institute for Bioengineering and Nanotechnology, and the University of Queensland Joint Research Scholarship.

Disclosure Statement

No competing financial interests exist.

References

1. Pittenger MF, AM Mackay, SC Beck, RK Jaiswal, R Douglas, JD Mosca, MA Moorman, DW Simonetti, S Craig and DR Marshak. (1999). Multilineage potential of adult human mesenchymal stem cells. Science 284:143–147.
2. Ren G, L Zhang, X Zhao, G Xu, Y Zhang, AI Roberts, RC Zhao and Y Shi. (2008). Mesenchymal stem cell-mediated immunosuppression occurs via concerted action of chemokines and nitric oxide. Cell Stem Cell 2:141–150.
3. Prockop DJ. (1997). Marrow stromal cells as stem cells for nonhematopoietic tissues. Science 276:71–74.
4. Takagi J. (2007). Structural basis for ligand recognition by integrins. Curr Opin Cell Biol 19:557–564.
5. Adams JC. (2001). Cell-matrix contact structures. Cell Mol Life Sci 58:371–392.
6. Hynes RO. (2002). Integrins: bidirectional, allosteric signaling machines. Cell 110:673–687.
7. Critchley DR. (2000). Focal adhesions—the cytoskeletal connection. Curr Opin Cell Biol 12:133–139.
8. Geiger B, JP Spatz and AD Bershadsky. (2009). Environmental sensing through focal adhesions. Nat Rev Mol Cell Biol 10:21–33.
9. Hynes RO. (1992). Integrins: versatility, modulation, and signaling in cell adhesion. Cell 69:11–25.
10. Legate KR and R Fassler. (2009). Mechanisms that regulate adaptor binding to beta-integrin cytoplasmic tails. J Cell Sci 122:187–198.
11. Riveline D, E Zamir, NQ Balaban, US Schwarz, T Ishizaki, S Narumiya, Z Kam, B Geiger and AD Bershadsky. (2001). Focal contacts as mechanosensors: externally applied local mechanical force induces growth of focal contacts by an mDia1-dependent and ROCK-independent mechanism. J Cell Biol 153:1175–1186.
12. Reference deleted.
13. Reference deleted.
14. Ishida T, TE Peterson, NL Kovach and BC Berk. (1996). MAP kinase activation by flow in endothelial cells. Role of beta 1 integrins and tyrosine kinases. Circ Res 79:310–316.
15. Wang JG, M Miyazu, E Matsushita, M Sokabe and K Naruse. (2001). Uniaxial cyclic stretch induces focal adhesion kinase (FAK) tyrosine phosphorylation followed by mitogen-activated protein kinase (MAPK) activation. Biochem Biophys Res Commun 288:356–361.
16. Eliceiri BP, R Klemke, S Stromblad and DA Cheresh. (1998). Integrin alphavbeta3 requirement for sustained mitogen-activated protein kinase activity during angiogenesis. J Cell Biol 140:1255–1263.
17. Gronthos S, PJ Simmons, SE Graves and PG Robey. (2001). Integrin-mediated interactions between human bone marrow stromal precursor cells and the extracellular matrix. Bone 28:174–181.
18. Klees RF, RM Salasznyk, K Kingsley, WA Williams, A Boskey and GE Plopper. (2005). Laminin-5 induces osteogenic gene expression in human mesenchymal stem cells through an ERK-dependent pathway. Mol Biol Cell 16:881–890.
19. Neuss S, E Becher, M Woltje, L Tietze and W Jahnen-Dechent. (2004). Functional expression of HGF and HGF receptor/c-met in adult human mesenchymal stem cells suggests a role in cell mobilization, tissue repair, and wound healing. Stem Cells 22:405–414.
20. Majumdar MK, V Banks, DP Peluso and EA Morris. (2000). Isolation, characterization, and chondrogenic potential of human bone marrow-derived multipotential stromal cells. J Cell Physiol 185:98–106.

21. Brooke G, H Tong, JP Levesque and K Atkinson. (2008). Molecular trafficking mechanisms of multipotent mesenchymal stem cells derived from human bone marrow and placenta. Stem Cells Dev 17:929–940.
22. Goessler UR, K Bieback, P Bugert, T Heller, H Sadick, K Hormann and F Riedel. (2006). *In vitro* analysis of integrin expression during chondrogenic differentiation of mesenchymal stem cells and chondrocytes upon dedifferentiation in cell culture. Int J Mol Med 17:301–307.
23. Goessler UR, P Bugert, K Bieback, J Stern-Straeter, G Bran, K Hormann and F Riedel. (2008). Integrin expression in stem cells from bone marrow and adipose tissue during chondrogenic differentiation. Int J Mol Med 21:271–279.
24. Loeser RF. (2000). Chondrocyte integrin expression and function. Biorheology 37:109–116.
25. Cheng SL, CF Lai, A Fausto, M Chellaiah, X Feng, KP McHugh, SL Teitelbaum, R Civitelli, KA Hruska, FP Ross and LV Avioli. (2000). Regulation of alphaVbeta3 and alphaVbeta5 integrins by dexamethasone in normal human osteoblastic cells. J Cell Biochem 77:265–276.
26. Hamidouche Z, O Fromigue, J Ringe, T Haupl, P Vaudin, JC Pages, S Srouji, E Livne and PJ Marie. (2009). Priming integrin alpha5 promotes human mesenchymal stromal cell osteoblast differentiation and osteogenesis. Proc Natl Acad Sci USA 106:18587–18591.
27. Liu J, SM DeYoung, M Zhang, M Zhang, A Cheng and AR Saltiel. (2005). Changes in integrin expression during adipocyte differentiation. Cell Metab 2:165–177.
28. Mauney J and V Volloch. (2009). Collagen I matrix contributes to determination of adult human stem cell lineage via differential, structural conformation-specific elicitation of cellular stress response. Matrix Biol 28:251–262.
29. Salasznyk RM, RF Klees, A Boskey and GE Plopper. (2007). Activation of FAK is necessary for the osteogenic differentiation of human mesenchymal stem cells on laminin-5. J Cell Biochem 100:499–514.
30. Salasznyk RM, RF Klees, MK Hughlock and GE Plopper. (2004). ERK signaling pathways regulate the osteogenic differentiation of human mesenchymal stem cells on collagen I and vitronectin. Cell Commun Adhes 11:137–153.
31. Salasznyk RM, WA Williams, A Boskey, A Batorsky and GE Plopper. (2004). Adhesion to vitronectin and collagen I promotes osteogenic differentiation of human mesenchymal stem cells. J Biomed Biotechnol 2004:24–34.
32. Doran MR, JE Frith, AB Prowse, J Fitzpatrick, EJ Wolvetang, TP Munro, PP Gray and JJ Cooper-White. (2010). Defined high protein content surfaces for stem cell culture. Biomaterials 31:5137–5142.
33. Mauney J and V Volloch. (2010). Human bone marrow-derived stromal cells show highly efficient stress-resistant adipogenesis on denatured collagen IV matrix but not on its native counterpart: implications for obesity. Matrix Biol 29:9–14.
34. Martino MM, M Mochizuki, DA Rothenfluh, SA Rempel, JA Hubbell and TH Barker. (2009). Controlling integrin specificity and stem cell differentiation in 2D and 3D environments through regulation of fibronectin domain stability. Biomaterials 30:1089–1097.
35. Mauney J and V Volloch. (2009). Progression of human bone marrow stromal cells into both osteogenic and adipogenic lineages is differentially regulated by structural conformation of collagen I matrix via distinct signaling pathways. Matrix Biol 28:239–250.
36. George PA, MR Doran, TI Croll, TP Munro and JJ Cooper-White. (2009). Nanoscale presentation of cell adhesive molecules via block copolymer self-assembly. Biomaterials 30: 4732–4737.
37. Hersel U, C Dahmen and H Kessler. (2003). RGD modified polymers: biomaterials for stimulated cell adhesion and beyond. Biomaterials 24:4385–4415.
38. Ruoslahti E. (1996). RGD and other recognition sequences for integrins. Annu Rev Cell Dev Biol 12:697–715.
39. Koivunen E, B Wang and E Ruoslahti. (1994). Isolation of a highly specific ligand for the alpha 5 beta 1 integrin from a phage display library. J Cell Biol 124:373–380.
40. Kibbey MC, M Jucker, BS Weeks, RL Neve, WE Van Nostrand and HK Kleinman. (1993). Beta-amyloid precursor protein binds to the neurite-promoting IKVAV site of laminin. Proc Nat Acad Sci USA 90:10150–10153.
41. Nomizu M, BS Weeks, CA Weston, WH Kim, HK Kleinman and Y Yamada. (1995). Structure-activity study of a laminin [alpha]1 chain active peptide segment Ile-Lys-Val-Ala-Val (IKVAV). FEBS Lett 365:227–231.
42. Freitas VM, VF Vilas-Boas, DC Pimenta, V Loureiro, MA Juliano, MR Carvalho, JJ Pinheiro, AC Camargo, AS Moriscot, MP Hoffman and RG Jaeger. (2007). SIKVAV, a laminin alpha1-derived peptide, interacts with integrins and increases protease activity of a human salivary gland adenoid cystic carcinoma cell line through the ERK 1/2 signaling pathway. Am J Pathol 171:124–138.
43. Maeda T, K Titani and K Sekiguchi. (1994). Cell-adhesive activity and receptor-binding specificity of the laminin-derived YIGSR sequence grafted onto Staphylococcal protein A. J Biochem 115:182–189.
44. Caniggia I, J Liu, R Han, J Wang, AK Tanswell, G Laurie and M Post. (1996). Identification of receptors binding fibronectin and laminin on fetal rat lung cells. Am J Physiol 270: L459–L468.
45. Hudson JE, JE Frith, BC Donose, E Rondeau, RJ Mills, EJ Wolvetang, GP Brooke and JJ Cooper-White. (2010). A synthetic elastomer based on acrylated polypropylene glycol triol with tunable modulus for tissue engineering applications. Biomaterials 31:7937–7947.
46. Majumdar MK, M Keane-Moore, D Buyaner, WB Hardy, MA Moorman, KR McIntosh and JD Mosca. (2003). Characterization and functionality of cell surface molecules on human mesenchymal stem cells. J Biomed Sci 10: 228–241.
47. Miura Y, M Miura, S Gronthos, MR Allen, C Cao, TE Uveges, Y Bi, D Ehirchiou, A Kortesidis, S Shi and L Zhang. (2005). Defective osteogenesis of the stromal stem cells predisposes CD18-null mice to osteoporosis. Proc Natl Acad Sci USA 102:14022–14027.
48. Semon JA, LH Nagy, CB Llamas, HA Tucker, RH Lee and DJ Prockop. (2010). Integrin expression and integrin-mediated adhesion *in vitro* of human multipotent stromal cells (MSCs) to endothelial cells from various blood vessels. Cell Tissue Res 341:147–158.
49. Gahmberg CG, M Tolvanen and P Kotovuori. (1997). Leukocyte adhesion—structure and function of human leukocyte beta2-integrins and their cellular ligands. Eur J Biochem 245:215–232.
50. Gronthos S, DM Franklin, HA Leddy, PG Robey, RW Storms and JM Gimble. (2001). Surface protein characterization of human adipose tissue-derived stromal cells. J Cell Physiol 189:54–63.
51. Goessler UR, P Bugert, K Bieback, H Sadick, A Baisch, K Hormann and F Riedel. (2006). *In vitro* analysis of differential expression of collagens, integrins, and growth factors in

cultured human chondrocytes. Otolaryngol Head Neck Surg 134:510–515.
52. Goessler UR, P Bugert, K Bieback, J Stern-Straeter, G Bran, H Sadick, K Hbrmann and F Riedel. (2009). *In vitro* analysis of integrin expression in stem cells from bone marrow and cord blood during chondrogenic differentiation. J Cell Mol Med 13:1175–1184.
53. Roca-Cusachs P, NC Gauthier, A Del Rio, and MP Sheetz. (2009). Clustering of alpha(5)beta(1) integrins determines adhesion strength whereas alpha(v)beta(3) and talin enable mechanotransduction. Proc Natl Acad Sci USA 106:16245–16250.
53a. Kundu AK, CB Khatiwala, and AJ Putnam. (2009). Extracellular matrix remodelling, integrin expression, and downstream signalling pathways influence the osteogenic differentiation of mesenchymal stem cells on poly(lactide-co-glycide) substrates. Tissue Eng Part A 15:273–283.
54. Studenovska H, M Slouf and F Rypacek. (2008). Poly (HEMA) hydrogels with controlled pore architecture for tissue regeneration applications. J Mater Sci: Mater Med 19: 615–621.
55. Duffy DC, JC McDonald, OJA Schueller and GM Whitesides. (1998). Rapid prototyping of microfluidic systems in poly (dimethylsiloxane). Anal Chem 70:4974–4984.
56. Wang Y, GA Ameer, BJ Sheppard and R Langer. (2002). A tough biodegradable elastomer. Nat Biotech 20:602–606.
57. Metters A and J Hubbell. (2005). Network formation and degradation behavior of hydrogels formed by Michael-type addition reactions. Biomacromolecules 6:290–301.
58. Aratani Y and Y Kitagawa. (1988). Enhanced synthesis and secretion of type IV collagen and entactin during adipose conversion of 3T3-L1 cells and production of unorthodox laminin complex. J Biol Chem 263:16163–16169.
59. Kubo Y, S Kaidzu, I Nakajima, K Takenouchi and F Nakamura. (2000). Organization of extracellular matrix components during differentiation of adipocytes in long-term culture. In Vitro Cell Dev Biol Anim 36:38–44.
60. Niimi T, C Kumagai, M Okano and Y Kitagawa. (1997). Differentiation-dependent expression of laminin-8 (alpha 4 beta 1 gamma 1) mRNAs in mouse 3T3-L1 adipocytes. Matrix Biol 16:223–230.
61. George PA, BC Donose and JJ Cooper-White. (2009). Self-assembling polystyrene-block-poly(ethylene oxide) copolymer surface coatings: resistance to protein and cell adhesion. Biomaterials 30:2449–2456.
62. Frith JE, RJ Mills and JJ Cooper-White. (2012). Lateral spacing of adhesion peptides influences human mesenchymal stem cell behaviour. J Cell Sci 125:317–327.
63. Reference deleted.
64. Reference deleted.
65. Tamada M, MP Sheetz and Y Sawada. (2004). Activation of a signaling cascade by cytoskeleton stretch. Dev Cell 7: 709–718.
66. Schallmoser K, E Rohde, A Reinisch, C Bartmann, D Thaler, C Drexler, AC Obenauf, G Lanzer, W Linkesch and D Strunk. (2008). Rapid large-scale expansion of functional mesenchymal stem cells from unmanipulated bone marrow without animal serum. Tissue Eng Part C: Methods 14:185–196.
67. Salasznyk RM, RF Klees, WA Williams, A Boskey and GE Plopper. (2007). Focal adhesion kinase signaling pathways regulate the osteogenic differentiation of human mesenchymal stem cells. Exp Cell Res 313:22–37.
68. Hausman GJ, JT Wright and RL Richardson. (1996). The influence of extracellular matrix substrata on preadipocyte development in serum-free cultures of stromal-vascular cells. J Anim Sci 74:2117–2128.
69. Schoenmakers RG, P van de Wetering, DL Elbert and JA Hubbell. (2004). The effect of the linker on the hydrolysis rate of drug-linked ester bonds. J Control Release 95: 291–300.
70. Spiegelman BM and CA Ginty. (1983). Fibronectin modulation of cell shape and lipogenic gene expression in 3t3-adipocytes. Cell 35:657–666.

Address correspondence to:
Prof. Justin John Cooper-White
Tissue Engineering and Microfluidics Laboratory
Australian Institute for Bioengineering and Nanotechnology
University of Queensland
St. Lucia, QLD 4072
Australia

E-mail: j.cooperwhite@uq.edu.au

Received for publication November 1, 2011
Accepted after revision March 26, 2012
Prepublished on Liebert Instant Online March 28, 2012